Neurology & Neuroscience

Original Article

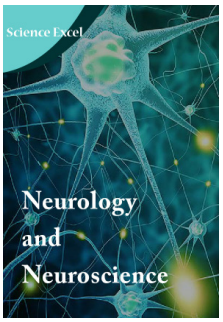

Cognitive Network Changes After Exposure to Haptic Vibrotactile Trigger Technology: Results From The ENHANCE Study

John J Haddad[1], Mark DeBrincat[2], Duane M North[3], Jay Dhaliwal[4], Peter Hurwitz[5]

[1]*Department of Biomedical Sciences, Faculty of Applied Sciences, American University of Technology, Byblos, Beirut, Lebanon*

[2]*Castle Rock, Colorado, USA*

[3]*EEG and Neuroimaging Laboratory, Applied Neuroscience Research Institute, St. Petersburg, FL, USA;*

[4]*Srysty Holdings Inc., Mississauga, ON, Canada*

[5]*Clarity Science LLC, Narragansett, Rhode Island, USA*

*Correspondence

Peter Hurwitz

Clarity Science LLC, 750 Boston Neck Road, Suite 11, Narragansett, RI 02882, USA

Tel: +1917 757 0521

Fax: +1855-891-8303

E-mail: peterh@claritysciences.org

- Received Date: 29 Aug 2023
- Accepted Date: 02 Sep 2023
- Publication Date: 08 Sep 2023

Keywords

EEG; Haptic Vibrotactile Trigger Technology, VTT, CBT; CNS; Cognition; eSmartr; HPT; LORETA; Neuropathology; PNS; qEEG; Somatosensory, ENHANCE study, Srysty Holdings Co., Cognitive Boost Technology, esmartr Smart Compression Sleeve.

Abstract

The conceptual framework of cognitive networks, or cognits, represents a system of working memory, especially long-term memory arrays that are intrinsically designed to attain certain behavioral ends and that are activated by a neural structure. Despite the fact that cognitions can be used in a plethora of systems, current technologies allow manipulations of the central nervous system (CNS) to execute certain sensory and motor functions.

Sensation and tactual perception by the skin are an innate mechanism for human survival and represent our adaptive somatosensorial ability to apprehend information via haptics—the active touch for object recognition and perception by higher centers of the brain. The somatosensation, which is identified by a set of channels and receptors sensitive to a variety of stimuli (thermal, tactile, and mechanical), is critical to survival, balance control, cognition, and pain modulation.

Cognits are cutting-edge tools and modalities that provide a landscape of theoretical assets, evidence-based experimental protocols, computational intelligence schemes, and direct empirical modalities that facilitate the understanding of the complex functionalities of the human brain.

By evaluating neuroimaging data after somatosensory stimulation and collected via electroencephalogram (EEG), cognition response and change can be obtained that allows researchers to gain a better understanding of emerging scientific approaches aimed at understanding human behavioral outcomes.

An emerging technology, haptic vibrotactile trigger technology (VTT), incorporates somatosensory patterns in compression sleeves. eSmartr Smart Compression Sleeves (Srysty Holdings Inc., Mississauga, ON, Canada) with VTT and its Cognitive Boost Technology (CBT) pattern is designed to optimize neural communications for improved mindful wellness. This technology has also been incorporated into patches, braces, apparel (socks), wrist bands, and other routes of delivery.

Mindful wellness is considered an outcome of somatosensory intervention that modulates the behavioral responses associated with cognitive networks. Currently, there is limited research exploring these modalities, exposing the need to study new technologies and their influence on somatosensory pathways and cognitive networks.

The purpose of this IRB-approved study was to explore the effects of forearm VTT stimulation patterns on cognitive networks by comparing a baseline EEG to an EEG after placing a sleeve incorporating VTT on the right or left forearm of adult healthy individuals.

Materials and methods: A baseline EEG was recorded over 5 minutes from 19 scalp locations on 20 subjects ranging in age from 17.6 years to 41.9 years (n=7 females, 13 males). The subject's dominant arm was then fitted with the eSmartr Smart Compression Sleeve for 20 minutes and another 5-minute EEG was recorded. Both the LORETA (*Low Resolution Electromagnetic Tomography Analysis*) inverse solution and a power spectral analysis of the surface EEG were calculated.

Additionally, for 10 distinct networks, the current sources from 88 Brodmann areas were computed. The variables were absolute power and absolute current density in 1 Hz increments in 10 frequency bands (delta, theta, alpha-1, alpha-2, beta-1, beta-2, beta-3, and hi-beta). Paired t-tests were computed for each individual for all EEG parameters, as well as group paired t-tests, between the baseline EEG and follow-up EEG.

Results: The results showed statistically significant t-test differences ($P < 0.01$) in both the surface EEG and the LORETA current sources between the baseline measurement and the follow-up 'sleeve-on' measurement. The largest differences were detected with a prominent downregulation of alpha and beta frequency powers at both the surface EEG and the LORETA current sources with the "sleeve-on," as

Citation: Haddad JJ, DeBrincat M, North DM, Dhaliwal J, Hurwitz P. Cognitive Network Changes After Exposure to Haptic Vibrotactile Trigger Technology: Results From The ENHANCE Study. Neurol Neurosci. 2023; 4(3):1-15.

compared to baseline.
In addition, the maximal effects of the "sleeve-on" condition were in the left frontal and left temporal surface EEGs and on the medial bank of the somatosensory cortex in the range of the alpha frequency. Changes in the default network and attention network were also prominent.
Conclusions*:* Study results indicate that these non-pharmacologic, non-invasive, haptic vibrotactile trigger technology (VTT) patterned compression sleeves elicited a response in multiple cognitive networks. These networks play a key role in executive function, memory, attention, mood, and information flow. There was a prominent effect of the haptic vibrotactile trigger technology with the CBT- patterned sleeves on the EEG that was primarily located in alpha and beta frequency bands. The substantial impacts on the homuncular projection of the arm to the medial somatosensory cortex as well as the default network demonstrated activity influenced by the patterned sleeve. The mechanisms of action of the VTT sleeve on the brain, neuropathways, and the EEG spectrum are still being investigated. If results are confirmed with further research, this novel VTT technology could be a promising addition as a non-invasive and non-drug treatment approach for a variety of conditions and therapeutic applications.

Introduction

Sensation and tactual perception by skin dermatomes and related neuro-receptors is an innate mechanism for human survival and regeneration of mindful wellness and represents our advanced and adaptive somatosensorial ability to apprehend information via haptics, which sustains the active touch for object recognition and perception by higher centers of the brain [1-6]. The somatosensation, which is distinguished by a collection of molecular receptors responsive to various stimuli (thermal, tactile, and mechanical), is essential for survival, balance regulation, pain modulation, and, more recently, cognitive networks and cerebral interactions [1,3,7,8].

The intricate peripheral and central nervous system (PNS/CNS) communications are crucial in determining sensory and motor outputs in response to various external and internal stimuli [9-11]. The cerebral cortex, in addition to the brain stem and cerebellum, in particular, play a critical role in sensory, motor, and integrative mechanisms, including human cognitive networks, commonly known as "cognitions" or "cognits" [4,12]. Cognits are invariant structural and functional architectures of brain neuronal networks that facilitate the integration of separate functions within unified modalities. Park and Friston [12] state that "context-sensitive integration during cognition tasks necessarily entails a divergence between structural and functional networks," even though functional networks are bound by structural connections. This application is crucial for understanding the nature of brain functioning in health and disease states [1,11].

The technology-based eSmartr approach, in evoking a pattern of integrated responses with these cognitions, incorporates haptic vibrotactile trigger technology (VTT) by targeting neurological cognitive networks that has been shown to elicit physiological and behavioral responses. VTT is designed to trigger skin receptors to generate a combination of sensory signals, which are subsequently processed by cognition after being relayed through neural modules, and theoretically leading to a natural 'reset' of the neural networks to enhance focus, clarity, and calmness. In theory, these neuro-signals represent a set of messages that may assist in amplification of cognitive abilities and awareness [1,6-8]. In recent years, haptic skin-stimulation technology has been incorporated into several over-the-counter products with different routes of delivery that include patches, apparel (socks), braces, wrist bands, and compression sleeves, among others [1,7,8,13].

Developed as a haptic vibrotactile trigger technology pattern, Cognitive Boost Technology (CBT) is a non-invasive, drug-free approach designed to improve cognition and interact with intricate communication pathways associated with the functionality of both the PNS and the CNS [7]. Specifically, it is believed that the compression present in the eSmartr Smart Compression Sleeve allows for the CBT pattern to activate dermatomes, thereby sending signals through somatosensory pathways to the CNS. This works in definitive ways, beginning with encoding, followed by filtering, and ending with decoding mechanisms. Sensory information is activated and encoded by specialized mechanoreceptors, which are a set of somatosensory receptors that convert extracellular signals to intracellular mechanisms associated with mechanically (tactile)-gated ion channels [1,3,7,8]. This VTT tactile stimulation used by the CBT pattern activates an encoded neuro-signal at the base of nerve receptors located on the forearm. It is subsequently communicated to central regions such as the entorhinal cortex, hippocampus, and prefrontal cortex by a system that filters sensory data at the brainstem level, segregating background interference or noise from meaningful information. This encoding-filtering pathway regulates neuro-processes within cognition, which in turn modulates certain functions, including the decoding (and enhancement) of decision-making centers, attention deficits, short- and long-term memory shortages, and information flow, segregation, and integration [1,7,8]. This is thought to subsequently lead to the cognizant regulation of working memory, cognitive flexibility and plasticity, and neuro-inhibitory control mechanisms generally associated with health and wellness. It is observed that these skills are critical for learning, problem-solving, and information processing. This module—the cognition-generated executive functions—that forms bridges between "network" and "cognitive" models could, in turn, be measured by EEG scans and related tomography [1,14-19]. The sensory pattern within the compression sleeve is in close symmetry between known EEG patterns and their role in modulating EEG and neuronal circuits within higher brain centers [1].

Unraveling the neuronal pathways and networks involved in cognitive control mechanisms is crucial in regenerative technology and neuropathology [1,5,7,8]. In addition, research has suggested that the impact of external stimulations or experimental interventions is likely to modulate those intricate webs of neuropathways [1,20].

With neuroimaging and advanced signal processing technologies, the optimization of cognitive networks requires topographically situated time-variant, waveform frequency-selective, and directed functional connectivity modules measurable by the EEG [1,21]. The Electroencephalogram (EEG) in its current application, and despite its limitations, is synonymous with mapping advances in neuronal activity [1].

Conventionally, kinematic measurements and neuroimaging techniques provide critical translational implications for diagnostic and prognostic criteria in several responses and approaches [1,3], recording brain activity by the EEG due to mechanical, cognitive, and sensory mechanisms related to somatosensory activation has confirmed intricate pathways and cortical networks that correlate with temporal and spatial paradigms [1,22,23].

A potential correlation has been established between EEG modulations and subsequent interference with neuronal activities within a system of cognits that are likely to be involved with specialized cognitive networks [1,24]. This may have neuropathological implications in the treatment of neurodegenerative diseases and deficit or debilitating conditions, in addition to enhancing the general wellness and functionality of the mindful individual [1,6,25].

The purpose of this non-invasive and minimal risk Institutional Review Board (IRB)-approved ENHANCE ("Evaluating Cognitive Network Response with Haptic Vibrotactile Trigger Technology - Neurological Changes via EEG Monitoring") Study was to explore the effects of forearm stimulation patterns on the EEG and cognitive networks by comparing a baseline EEG to an EEG after placing a VTT-patterned sleeve on the right or left forearm of healthy individuals.

Methods

Study Design

This study was a prospective, Institutional Review Board-approved Study in healthy volunteers comparing a baseline EEG with an EEG after placement of a haptic vibrotactile trigger technology (VTT) embedded compression sleeve (eSmartr Smart Compression Sleeve) on the right or left forearm (See Figure 1).

Subjects

A total population group of 20 subjects, ranging in age from 17.6 to 41.9 years (n = 7 females, 13 males) were recruited into the study and whose health at the time of enrollment was normal according to their medical histories. After consenting, the patterned eSmartr Smart Compression sleeve was placed on the dominantly used arm as preferentially defined by the subject's handedness (n = 4 left arm, 16 right arm).

Figure 1. *eSmartr Smart Compression Sleeve*

Study procedures and assessments

EEG Recordings

While in a sitting position, the individuals were instructed to sit, remain still, and keep their eyes closed for approximately five minutes while the baseline EEG was recorded. The EEG data collected from 19 scalp electrodes in accordance with the International 10/20 electrode locations was amplified and digitalized using the Wearable Sensing DSI-24 dry amplifier device system. Approximately 2–5 minutes of EEG were recorded in the eyes-closed condition, with subjects sitting at rest with no sleeves on their arms (control group, n = 20). After placing the sleeve on each subject's dominant arm (n = 20), and waiting approximately 20- minutes, a second, 2–5 minute EEG recording in the eyes-closed condition was taken. The time lapse between the two groups was determined to be statistically insignificant.

LORETA Current density Measurement and Statistical analysis

LORETA current density

The currents at the three-dimensional gray matter voxels "J" in LORETA, a distributed EEG inverse solution, are a linear combination of the signal "S" recorded at a scalp electrode, as follows:

$$J = T \times S$$

where "T" is a minimum-normal three-dimensional matrix made up of 2,394 gray matter voxels with x, y, and z coordinates in a generalized inverse that gives more weight to sources that are synchronous in surrounding volumes or regions [26]. The "T" matrix is described mathematically as follows:

where "B" is the discrete Laplacian Operator and "W" is a weighting matrix (inv indicates inverse), and pinv(X) is the "Moore-Penrose pseudoinverse of X" [27,28].

The Talairach Atlas coordinates of the Montreal Neurological Institute's magnetic resonance imaging (MRI) average of 305 brains [26,29]. and the linkage to standard anatomical 7 mm x 7 mm x 7 mm voxels, each with a distinct Talairach Atlas coordinate. Groups of voxels are also defined by the clear anatomical landmarks established by von Brodmann in 1909 and referred to as Brodmann areas [30,31]. The square root of the sum of the squares for the x, y, and z source moments for each 0.5 Hz frequency band was used to construct the resultant current source vector at each voxel. To minimize the number of variables, each of the 2,394 gray matter voxels had adjacent 0.5 Hz bins averaged to form 1 Hz bins ranging from 1 Hz to 40 Hz.

$$T = \{inv(WB'BW)\}K'\{pinv(WB'BW)K'\}$$

For all variables, descriptive statistics were calculated, including frequencies and percent for categorical variables and means with standard deviation (SD) for continuous variables. The maximum sample size available was used for each statistical analysis.

A two-tailed alpha was set to 0.05 for all statistical comparisons. SPSS v. 27 was used for all analyses.

All experimental methods reported are consistent with international standards and regulations governing higher academic research relating to the integrity of handling human subjects, whose consents have been independently registered and verified. The wellbeing of experimental individuals has been ensured throughout the experimentation process.

The study was approved by an institutional review board and was performed in full accordance with the rules of the Health Insurance Portability and Accountability Act of 1996 (HIPAA) and the principles of the declaration of Helsinki and the international council of Harmonisation/GCP. All patients gave informed and written consent.

Results

Surface EEG Paired t-Tests

Table-1 and the topographic maps presented in Figure-2 demonstrate the results of the surface EEG paired t-tests comparing the baseline EEG and the EEG obtained during the post-sleeve condition according to different frequency bands. The largest differences were in the left hemisphere, particularly in the alpha frequency band (8–12 Hz).

As shown in Figure-3, there are EEG coherence paired t-tests that demonstrated noticeable reduced connectivity in the left hemisphere and elevated coherence in the right hemisphere, especially in the alpha frequency band.

Table 1. *The outcomes of the 19-channel surface EEG's paired t-tests comparing the baseline EEG and the post-sleeve condition EEG. The strongest effects were reduced power in the alpha frequency band (8–12 Hz), especially in the left hemisphere.*

FFT Absolute Power Group Paired t-Test (P-Value)

Intrahemispheric: LEFT

	DELTA	THETA	ALPHA	BETA	HIGH BETA	BETA 1	BETA 2	BETA 3
FP1 - LE	0.040	0.828	0.059	0.377	0.674	0.413	0.576	0.658
F3 - LE	0.873	0.231	0.004	0.086	0.198	0.146	0.237	0.089
C3 - LE	0.634	0.209	0.005	0.462	0.503	0.843	0.288	0.240
P3 - LE	0.752	0.474	0.047	0.453	0.925	0.381	0.596	0.772
O1 - LE	0.737	0.286	0.017	0.881	0.102	0.724	0.894	0.568
F7 - LE	0.064	0.148	0.037	0.192	0.961	0.582	0.279	0.151
T3 - LE	0.523	0.765	0.254	0.974	0.778	0.785	0.895	0.694
T5 - LE	0.725	0.333	0.014	0.216	0.589	0.177	0.213	0.623

Intrahemispheric: RIGHT

	DELTA	THETA	ALPHA	BETA	HIGH BETA	BETA 1	BETA 2	BETA 3
FP2 - LE	0.014	0.422	0.047	0.269	0.382	0.332	0.225	0.599
F4 - LE	0.557	0.590	0.069	0.303	0.731	0.196	0.621	0.818
C4 - LE	0.842	0.439	0.051	0.304	0.931	0.164	0.524	0.601
P4 - LE	0.507	0.337	0.082	0.621	0.858	0.601	0.592	0.794
O2 - LE	0.785	0.813	0.050	0.875	0.195	0.740	0.724	0.980
F8 - LE	0.020	0.238	0.087	0.346	0.732	0.506	0.287	0.511
T4 - LE	0.080	0.035	0.002	0.046	0.821	0.027	0.056	0.111
T6 - LE	0.279	0.147	0.011	0.134	0.831	0.145	0.076	0.149

Intrahemispheric: CENTER

	DELTA	THETA	ALPHA	BETA	HIGH BETA	BETA 1	BETA 2	BETA 3
Fz - LE	0.470	0.038	0.002	0.012	0.065	0.007	0.025	0.031
Cz - LE	0.197	0.227	0.019	0.152	0.187	0.112	0.286	0.467
Pz - LE	0.829	0.959	0.262	0.772	0.512	0.741	0.714	0.689

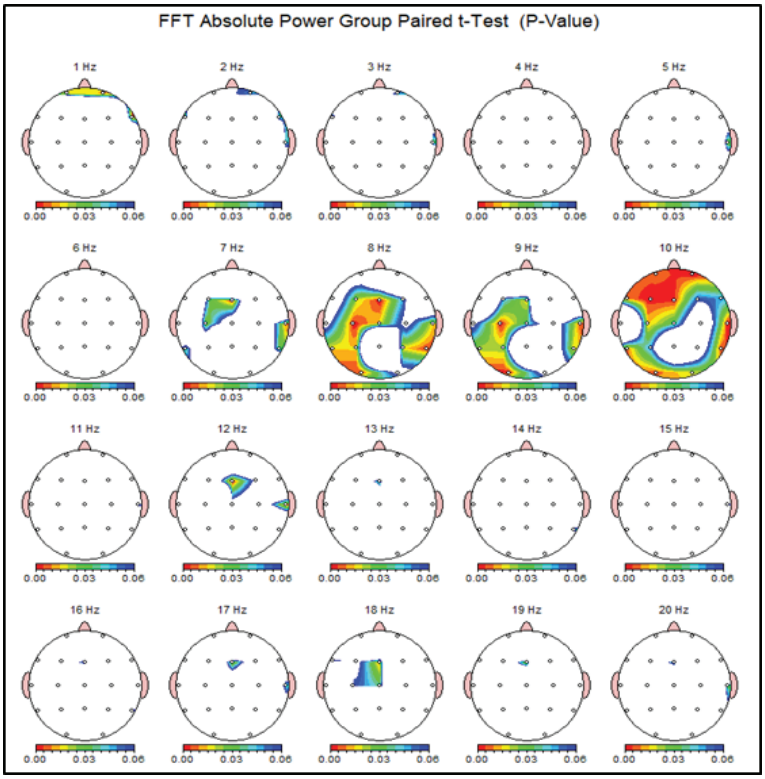

Figure 2. *Topographic maps of paired t-tests obtained from the 19-channel surface EEG between the baseline and post-sleeve conditions. The strongest effects were reduced power in the alpha frequency band (8–12 Hz), especially in the left central and frontal regions.*

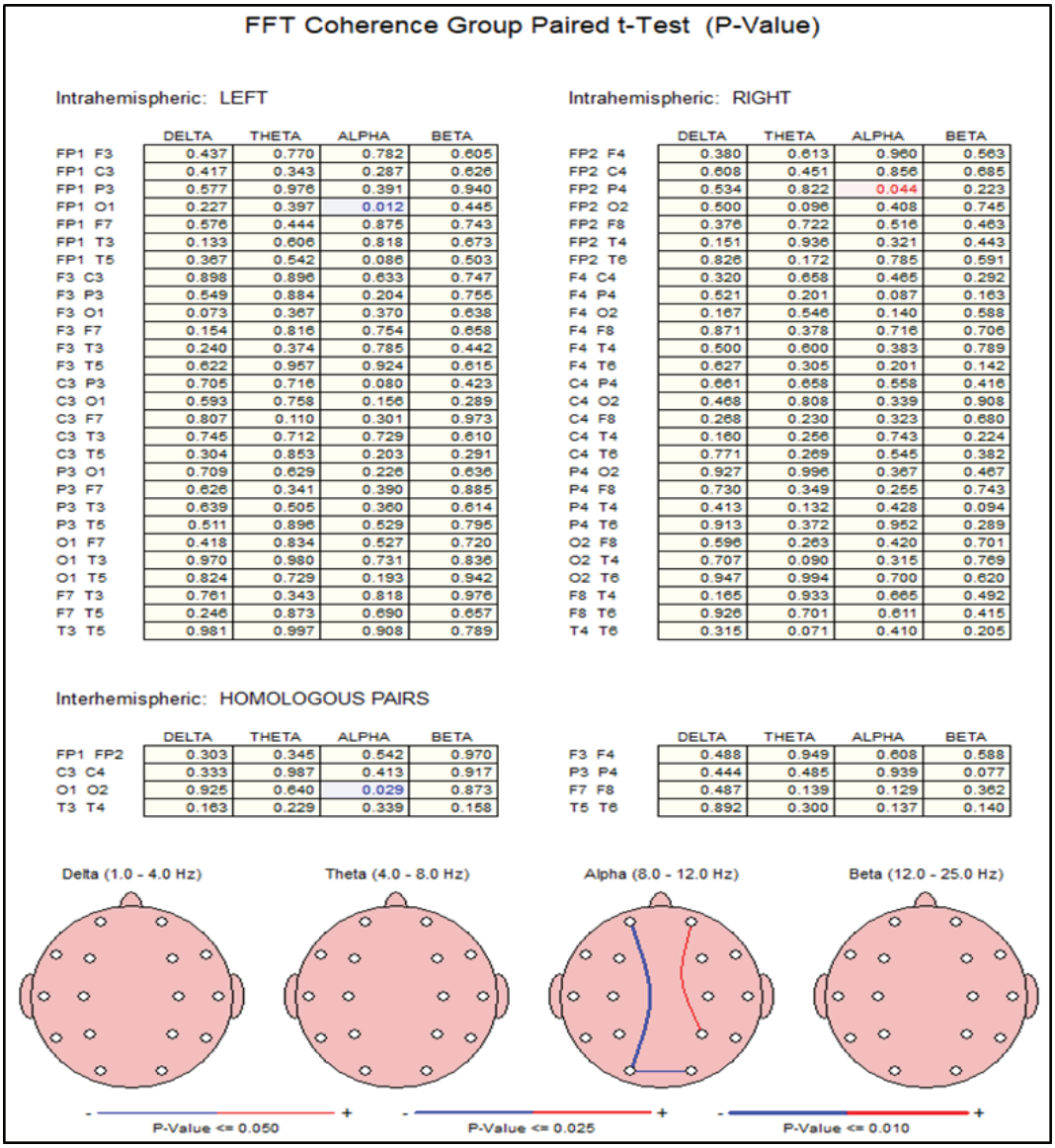

Intrahemispheric: LEFT	DELTA	THETA	ALPHA	BETA
FP1 F3	0.437	0.770	0.782	0.605
FP1 C3	0.417	0.343	0.287	0.626
FP1 P3	0.577	0.976	0.391	0.940
FP1 O1	0.227	0.397	0.012	0.445
FP1 F7	0.576	0.444	0.875	0.743
FP1 T3	0.133	0.606	0.818	0.673
FP1 T5	0.367	0.542	0.086	0.503
F3 C3	0.898	0.896	0.633	0.747
F3 P3	0.549	0.884	0.204	0.755
F3 O1	0.073	0.367	0.370	0.638
F3 F7	0.154	0.816	0.754	0.658
F3 T3	0.240	0.374	0.785	0.442
F3 T5	0.622	0.957	0.924	0.615
C3 P3	0.705	0.716	0.080	0.423
C3 O1	0.593	0.758	0.156	0.289
C3 F7	0.807	0.110	0.301	0.973
C3 T3	0.745	0.712	0.729	0.610
C3 T5	0.304	0.853	0.203	0.291
P3 O1	0.709	0.629	0.226	0.636
P3 F7	0.626	0.341	0.390	0.885
P3 T3	0.639	0.505	0.360	0.614
P3 T5	0.511	0.896	0.529	0.795
O1 F7	0.418	0.834	0.527	0.720
O1 T3	0.970	0.980	0.731	0.836
O1 T5	0.824	0.729	0.193	0.942
F7 T3	0.761	0.343	0.818	0.976
F7 T5	0.246	0.873	0.690	0.657
T3 T5	0.981	0.997	0.908	0.789

Intrahemispheric: RIGHT	DELTA	THETA	ALPHA	BETA
FP2 F4	0.380	0.613	0.960	0.563
FP2 C4	0.608	0.451	0.856	0.685
FP2 P4	0.534	0.822	0.044	0.223
FP2 O2	0.500	0.096	0.408	0.745
FP2 F8	0.376	0.722	0.516	0.463
FP2 T4	0.151	0.936	0.321	0.443
FP2 T6	0.826	0.172	0.785	0.591
F4 C4	0.320	0.658	0.465	0.292
F4 P4	0.521	0.201	0.087	0.163
F4 O2	0.167	0.546	0.140	0.588
F4 F8	0.871	0.378	0.716	0.706
F4 T4	0.500	0.600	0.383	0.789
F4 T6	0.627	0.305	0.201	0.142
C4 P4	0.661	0.658	0.558	0.416
C4 O2	0.468	0.808	0.339	0.908
C4 F8	0.268	0.230	0.323	0.680
C4 T4	0.160	0.256	0.743	0.224
C4 T6	0.771	0.269	0.545	0.382
P4 O2	0.927	0.996	0.367	0.467
P4 F8	0.730	0.349	0.255	0.743
P4 T4	0.413	0.132	0.428	0.094
P4 T6	0.913	0.372	0.952	0.289
O2 F8	0.596	0.263	0.420	0.701
O2 T4	0.707	0.090	0.315	0.769
O2 T6	0.947	0.994	0.700	0.620
F8 T4	0.165	0.933	0.665	0.492
F8 T6	0.926	0.701	0.611	0.415
T4 T6	0.315	0.071	0.410	0.205

Interhemispheric: HOMOLOGOUS PAIRS	DELTA	THETA	ALPHA	BETA
FP1 FP2	0.303	0.345	0.542	0.970
C3 C4	0.333	0.987	0.413	0.917
O1 O2	0.925	0.640	0.029	0.873
T3 T4	0.163	0.229	0.339	0.158

	DELTA	THETA	ALPHA	BETA
F3 F4	0.488	0.949	0.608	0.588
P3 P4	0.444	0.485	0.939	0.077
F7 F8	0.487	0.139	0.129	0.362
T5 T6	0.892	0.300	0.137	0.140

Figure 3. *The EEG coherence paired t-tests demonstrated reduced connectivity in the left hemisphere and elevated connectivity in the right hemisphere in the alpha frequency band.*

LORETA Current Density

The outcomes of paired t-tests for LORETA current density in the eyes-closed condition between baseline and sleeves-on are displayed in Table-2. The effects appeared to be widespread, with statistically significant differences ($P < 0.05$) in all Brodmann areas except for right hemisphere BA 44, BA 45, and BA 46. The statistical effect size was greater in the left hemisphere compared to the right. The alpha frequency band had more statistically significant differences than other frequency bands.

According to Figure-4, the results show paired t-tests between the baseline EEG and the EEG recorded after wearing the patterned sleeve. The magnetic resonance imaging (MRI) slices are 7 mm thick and are sequentially displayed, starting at the lowest slice (top left) and advancing in 15 steps to the upper MRI cortical regions. Bilaterally significant differences were present, especially in the frontal and temporal lobes and the midline areas of the default network hubs, with the largest effects on the medial banks of the two hemispheres.

Figure-5 shows a comparison of cortical current densities between the baseline EEG and the EEG recorded during the post-sleeve condition, with paired t-test values ranging from $P < 0.05$ to $P < 0.0001$. Bilaterally significant differences were present. The bilateral frontal lobes, including the sensory motor strip on the dorsal surface as well as the medial wall of the somatosensory projection regions of the arm (homunculus), are shown at 10 Hz.

Brain Networks

Table-3 shows the list of Brodmann areas that comprised the regions of interest for the 10 networks. The Brodmann areas that comprise a given network are based on the functional magnetic resonance imaging (fMRI) and positron emission tomography (PET). [16,32].

Table-4 shows the percentage of subjects who showed statistically significant differences between the baseline EEG and the EEG obtained with the sleeve using group paired t-tests. The alpha frequency demonstrated the strongest effects, where

Left Hemisphere	Delta	Theta	Alpha	Beta	High Beta	Alpha 1	Alpha 2	Beta 1	Beta 2	Beta 3
Brodmann Area	1.0 - 4.0 Hz	4.0 - 8.0 Hz	8.0 - 12.0 Hz	12.0 - 25.0 Hz	25.0 - 30.0 Hz	8.0 - 10.0 Hz	10.0 - 12.0 Hz	12.0 - 15.0 Hz	15.0 - 18.0 Hz	18.0 - 25.0 Hz
BA1	0.3136	0.2703	0.0236	0.1261	0.0914	0.0236	0.0236	0.1836	0.1261	0.1261
BA2	0.3337	0.2905	0.0248	0.1324	0.1076	0.0248	0.0248	0.2861	0.1324	0.1324
BA3	0.2839	0.2462	0.0200	0.1184	0.0880	0.0200	0.0200	0.1399	0.1184	0.1184
BA4	0.1393	0.1279	0.0159	0.0448	0.0953	0.0159	0.0159	0.0828	0.1219	0.0448
BA5	0.1146	0.1038	0.0178	0.0841	0.2731	0.0178	0.0178	0.0841	0.2034	0.2209
BA6	0.0799	0.0533	0.0009	0.0244	0.0954	0.0009	0.0009	0.0350	0.0778	0.0244
BA7	0.1122	0.1089	0.0185	0.0845	0.2744	0.0185	0.0185	0.0845	0.1992	0.2090
BA8	0.1152	0.0611	0.0084	0.0722	0.1170	0.0084	0.0084	0.1654	0.1412	0.0722
BA9	0.1221	0.0753	0.0350	0.0853	0.1161	0.0350	0.0350	0.1478	0.1298	0.0853
BA10	0.0995	0.0672	0.0218	0.0264	0.1330	0.0218	0.0218	0.0264	0.0971	0.0656
BA11	0.0963	0.0963	0.0390	0.0584	0.1974	0.0390	0.0390	0.1499	0.1965	0.0584
BA13	0.2647	0.0561	0.0007	0.0085	0.1012	0.0007	0.0007	0.0350	0.0923	0.0085
BA17	0.2862	0.3644	0.2501	0.2675	0.2336	0.2501	0.2501	0.3244	0.2675	0.2675
BA18	0.2293	0.2985	0.0769	0.1855	0.2067	0.0769	0.0769	0.2752	0.2341	0.1855
BA19	0.1398	0.2043	0.0398	0.1610	0.2064	0.0398	0.0398	0.1610	0.2472	0.1928
BA20	0.1970	0.0508	0.0010	0.0261	0.1694	0.0010	0.0010	0.1344	0.1534	0.0261
BA21	0.1295	0.0782	0.0030	0.0086	0.1450	0.0030	0.0030	0.0607	0.0981	0.0086
BA22	0.1255	0.0779	0.0075	0.0211	0.1433	0.0075	0.0075	0.0561	0.1681	0.0211
BA23	0.0850	0.0271	0.0012	0.0124	0.1550	0.0012	0.0012	0.0124	0.0764	0.0861
BA24	0.0812	0.0263	0.0010	0.0144	0.0739	0.0010	0.0010	0.0144	0.0645	0.0662
BA25	0.2757	0.0705	0.0048	0.0439	0.2031	0.0048	0.0048	0.0439	0.1310	0.0641
BA27	0.4270	0.0562	0.0061	0.2477	0.3276	0.0061	0.0061	0.2571	0.2477	0.3157
BA28	0.3339	0.0497	0.0017	0.0357	0.1862	0.0017	0.0017	0.0902	0.1168	0.0357
BA29	0.2630	0.0795	0.0021	0.1052	0.1089	0.0021	0.0021	0.1059	0.1527	0.1052
BA30	0.2831	0.0509	0.0056	0.2358	0.2009	0.0056	0.0056	0.2523	0.2358	0.2763
BA31	0.0793	0.0484	0.0009	0.0244	0.1491	0.0009	0.0009	0.0244	0.0766	0.1003
BA32	0.1374	0.0448	0.0109	0.0247	0.0929	0.0109	0.0109	0.0247	0.0955	0.0667
BA33	0.1572	0.0382	0.0161	0.0861	0.0917	0.0161	0.0161	0.1133	0.1321	0.0861
BA34	0.3114	0.0652	0.0034	0.0298	0.1750	0.0034	0.0034	0.0395	0.1303	0.0298
BA35	0.3361	0.0346	0.0011	0.0362	0.1940	0.0011	0.0011	0.1090	0.1068	0.0362
BA36	0.3341	0.0396	0.0012	0.0367	0.1917	0.0012	0.0012	0.1027	0.1502	0.0367
BA37	0.2927	0.0613	0.0034	0.0384	0.1943	0.0034	0.0034	0.0534	0.1264	0.0384
BA38	0.2539	0.1319	0.0174	0.0259	0.1628	0.0174	0.0174	0.0672	0.1864	0.0259
BA39	0.3086	0.2472	0.0391	0.1641	0.2801	0.0391	0.0391	0.1941	0.3237	0.1641
BA40	0.2647	0.1633	0.0080	0.0915	0.0945	0.0080	0.0080	0.1198	0.1289	0.0915
BA41	0.1682	0.1073	0.0018	0.0925	0.1041	0.0018	0.0018	0.1068	0.1502	0.0925
BA42	0.1510	0.1367	0.0112	0.0842	0.1227	0.0112	0.0112	0.1278	0.1931	0.0842
BA43	0.2545	0.2061	0.0096	0.0983	0.1021	0.0096	0.0096	0.1261	0.1461	0.0983
BA44	0.2881	0.1218	0.0161	0.0136	0.1296	0.0161	0.0161	0.0493	0.1394	0.0136
BA45	0.2267	0.1638	0.0616	0.0406	0.1284	0.0616	0.0616	0.0889	0.1248	0.0406
BA46	0.1941	0.1801	0.0703	0.0783	0.1260	0.0703	0.0703	0.1341	0.1392	0.0783
BA47	0.2974	0.1380	0.0204	0.0347	0.1620	0.0204	0.0204	0.0570	0.1614	0.0347
Amygdala	0.3360	0.0617	0.0029	0.0262	0.1696	0.0029	0.0029	0.0654	0.1221	0.0262
Hippocampus	0.3364	0.0356	0.0011	0.0335	0.1896	0.0011	0.0011	0.0908	0.1171	0.0335

Right Hemisphere	Delta	Theta	Alpha	Beta	High Beta	Alpha 1	Alpha 2	Beta 1	Beta 2	Beta 3
Brodmann Area	1.0 - 4.0 Hz	4.0 - 8.0 Hz	8.0 - 12.0 Hz	12.0 - 25.0 Hz	25.0 - 30.0 Hz	8.0 - 10.0 Hz	10.0 - 12.0 Hz	12.0 - 15.0 Hz	15.0 - 18.0 Hz	18.0 - 25.0 Hz
BA1	0.0916	0.1645	0.0332	0.1501	0.2754	0.0332	0.0332	0.2524	0.1857	0.1501
BA2	0.0965	0.1721	0.0352	0.1562	0.2817	0.0352	0.0352	0.2623	0.1886	0.1562
BA3	0.0758	0.0978	0.0126	0.1217	0.2428	0.0126	0.0126	0.1445	0.1496	0.1217
BA4	0.0825	0.0803	0.0189	0.0510	0.2072	0.0189	0.0189	0.0510	0.1247	0.0748
BA5	0.1307	0.1042	0.0143	0.0689	0.2713	0.0143	0.0143	0.0689	0.2094	0.1982
BA6	0.0800	0.0439	0.0009	0.0282	0.0955	0.0009	0.0009	0.0282	0.0785	0.0551
BA7	0.1298	0.1120	0.0181	0.0870	0.2602	0.0181	0.0181	0.0870	0.1924	0.2290
BA8	0.1205	0.0614	0.0086	0.0969	0.1175	0.0086	0.0086	0.1627	0.1489	0.0969
BA9	0.1096	0.0747	0.0361	0.0885	0.1241	0.0361	0.0361	0.1386	0.1496	0.0885
BA10	0.1067	0.0540	0.0237	0.0253	0.1626	0.0237	0.0237	0.0253	0.0925	0.0718
BA11	0.1182	0.1227	0.0470	0.1420	0.2438	0.0470	0.0470	0.1420	0.2291	0.1538
BA13	0.0794	0.0157	0.0013	0.0194	0.1845	0.0013	0.0013	0.0194	0.0534	0.0468
BA17	0.2878	0.3845	0.2458	0.2848	0.2368	0.2458	0.2458	0.3259	0.2960	0.2848
BA18	0.2085	0.1915	0.1152	0.2227	0.2136	0.1152	0.1152	0.2420	0.2227	0.2454
BA19	0.1769	0.0831	0.0213	0.1100	0.2036	0.0213	0.0213	0.1288	0.1100	0.2129
BA20	0.0210	0.0071	0.0002	0.0043	0.1025	0.0002	0.0002	0.0043	0.0273	0.0126
BA21	0.0179	0.0049	0.0002	0.0073	0.1262	0.0002	0.0002	0.0073	0.0242	0.0140
BA22	0.0182	0.0055	0.0002	0.0070	0.1257	0.0002	0.0002	0.0070	0.0263	0.0151
BA23	0.0833	0.0272	0.0012	0.0124	0.1551	0.0012	0.0012	0.0124	0.0767	0.0865
BA24	0.0798	0.0263	0.0010	0.0144	0.0739	0.0010	0.0010	0.0144	0.0647	0.0690
BA25	0.2622	0.0681	0.0069	0.0553	0.2097	0.0069	0.0069	0.0553	0.1448	0.0938
BA27	0.2463	0.0772	0.0333	0.1895	0.4021	0.0333	0.0333	0.1895	0.2360	0.3086
BA28	0.2979	0.0285	0.0047	0.0657	0.2218	0.0047	0.0047	0.0657	0.1522	0.1241
BA29	0.0663	0.0150	0.0009	0.0410	0.1861	0.0009	0.0009	0.0410	0.0727	0.0865
BA30	0.2474	0.1233	0.0276	0.2288	0.1974	0.0276	0.0276	0.2811	0.3095	0.2288
BA31	0.0791	0.0484	0.0009	0.0247	0.1492	0.0009	0.0009	0.0247	0.0767	0.1005
BA32	0.1364	0.0402	0.0106	0.0255	0.0868	0.0106	0.0106	0.0255	0.0931	0.0693
BA33	0.1576	0.0375	0.0154	0.0857	0.0912	0.0154	0.0154	0.1105	0.1309	0.0857
BA34	0.3093	0.0550	0.0087	0.0923	0.2416	0.0087	0.0087	0.0923	0.2160	0.1262
BA35	0.2415	0.0105	0.0034	0.0440	0.1845	0.0034	0.0034	0.0440	0.0969	0.1060
BA36	0.1098	0.0169	0.0026	0.0226	0.1325	0.0026	0.0026	0.0226	0.0480	0.0522
BA37	0.0681	0.0108	0.0004	0.0167	0.1363	0.0004	0.0004	0.0167	0.0252	0.0237
BA38	0.1192	0.0379	0.0272	0.0505	0.2478	0.0272	0.0272	0.0505	0.0777	0.0789
BA39	0.1884	0.0761	0.0297	0.0902	0.2180	0.0297	0.0297	0.1036	0.0902	0.2563
BA40	0.0454	0.0221	0.0016	0.0419	0.1893	0.0016	0.0016	0.0419	0.0635	0.0714
BA41	0.0377	0.0084	0.0010	0.0211	0.1556	0.0010	0.0010	0.0211	0.0325	0.0459
BA42	0.0232	0.0065	0.0004	0.0118	0.1442	0.0004	0.0004	0.0118	0.0393	0.0297
BA43	0.0471	0.0568	0.0035	0.0433	0.1864	0.0035	0.0035	0.0433	0.1081	0.0686
BA44	0.1077	0.0671	0.0661	0.0709	0.2334	0.0661	0.0661	0.1199	0.1528	0.0709
BA45	0.1187	0.1075	0.1119	0.1064	0.2586	0.1119	0.1119	0.2751	0.2751	0.1064
BA46	0.1347	0.1416	0.1449	0.2125	0.3050	0.1449	0.1509	0.3571	0.3648	0.2125
BA47	0.0976	0.0665	0.0363	0.1413	0.2731	0.0363	0.0363	0.1917	0.2843	0.1413
Amygdala	0.3073	0.0611	0.0103	0.0949	0.2473	0.0103	0.0103	0.0949	0.1880	0.1322
Hippocampus	0.2366	0.0187	0.0033	0.0364	0.1713	0.0033	0.0033	0.0364	0.0824	0.0967

Table 2. *Group paired t-test results for LORETA current source density between the baseline EEG and the post-sleeve EEG in all frequency bands and all Brodmann areas.*

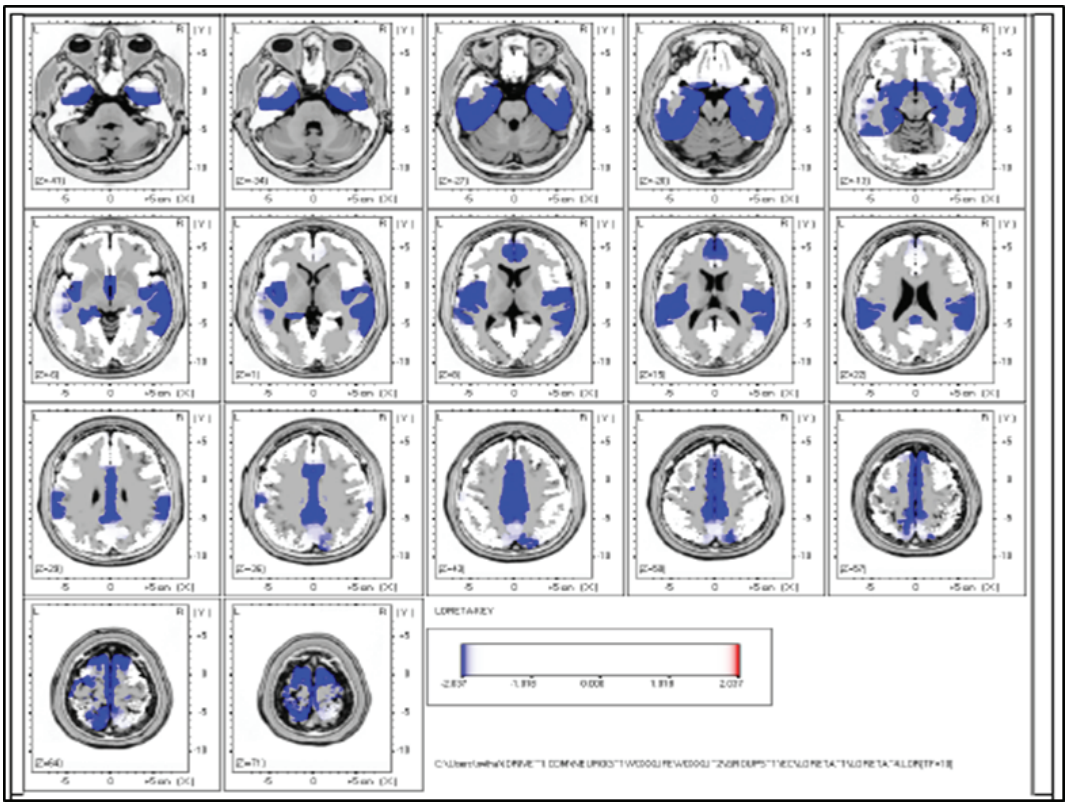

Figure 4. *Group paired t-test results for LORETA current source density between the baseline EEG and the post-sleeve EEG in all frequency bands and all Brodmann areas.*

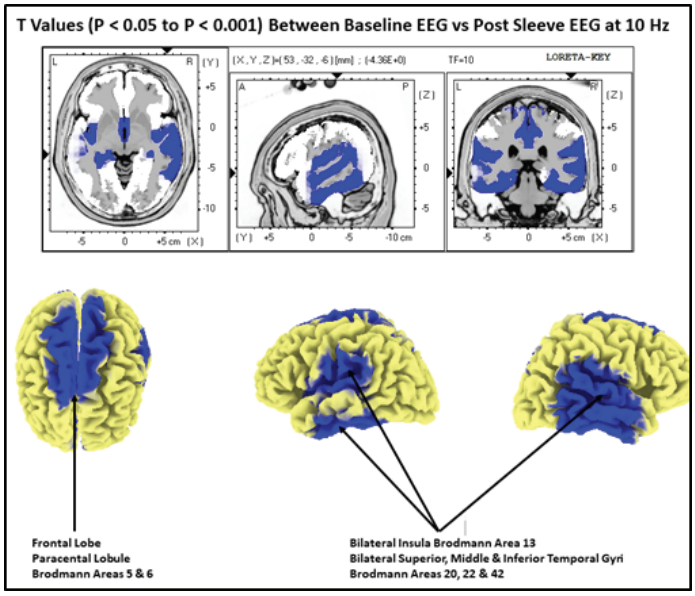

Figure 5. *Paired t-test (P < 0.05 to P < 0.0001) differences in current density between the baseline EEG and the EEG recorded during the post-sleeve condition.*

Table 3. *List of the Brodmann areas that comprise regions of interest (lobular regions) and related networks.*

Lobular Regions				Networks											
FRONTAL	TEMPORAL	PARIETAL	OCCIPITAL	Pain	Attn Dorsal	Attn Ventral	Default Mode	Reward	Mood	Work Mem	Anxiety	Executive	Fr-Occ	Facial Rec
BA4	BA13	BA1	BA17	BA1	BA6	BA10	BA2	BA8	BA10	BA7	BA4	BA5	BA8	BA7
BA6	BA20	BA2	BA18	BA2	BA7	BA11	BA7	BA9	BA11	BA8	BA6	BA7	BA9	BA9
BA8	BA21	BA3	BA19	BA3	BA8	BA19	BA10	BA10	BA13	BA9	BA7	BA8	BA10	BA10
BA9	BA22	BA5		BA4	BA9	BA21	BA11	BA24	BA23	BA24	BA10	BA9	BA11	BA11
BA10	BA27	BA7		BA5	BA19	BA37	BA19	BA30	BA24	BA30	BA13	BA10	BA17	BA17
BA11	BA28	BA23		BA13	BA39	BA44	BA29	BA32	BA32	BA31	BA21	BA11	BA18	BA18
BA24	BA29	BA31		BA24	BA40	BA45	BA30	BA33	BA33	BA32	AMYG	BA46	BA19	BA19
BA25	BA30	BA39		BA32		AMYG	BA31	BA44	BA44	BA33		BA47	BA37	BA20
BA32	BA34	BA40		BA33			BA35	BA45	BA45	BA40			BA45	BA21
BA33	BA35	BA43					BA39	BA47	BA47	HIPP			BA46	BA27
BA44	BA36						BA40	AMYG						BA38
BA45	BA37							HIPP						BA40
BA46	BA38													
BA47	BA41													
	BA42													
	Amygdala													
	Hippocampus													

Table 4. *List of subjects showing statistically significant variations in lobules and brain networks between baseline EEG and EEG recorded with a sleeve on the forearm. The alpha-frequency band exhibited the strongest effects.*

% of Significant T-TESTs Brodmann Areas per LORETA Network @ p<=.05										
LORETA Eyes Closed		DELTA	THETA	ALPHA	BETA	HI-BETA	ALPHA1	ALPHA2	BETA1	BETA2	BETA3
LOBEs:	FRONTAL	0%	25%	82%	46%	0%	82%	82%	36%	0%	18%
	TEMPORAL	15%	50%	100%	68%	0%	100%	100%	38%	21%	56%
	PARIETAL	10%	25%	100%	30%	0%	100%	100%	30%	0%	0%
	OCCIPITAL	0%	0%	33%	0%	0%	33%	33%	0%	0%	0%
NETWORKs:	Pain	0%	39%	100%	39%	0%	100%	100%	33%	0%	17%
	Attn Dorsal	7%	14%	100%	21%	0%	100%	100%	21%	0%	7%
	Attn Ventral	6%	13%	81%	56%	0%	81%	81%	31%	13%	44%
	Default Mode	5%	27%	100%	36%	0%	100%	100%	32%	0%	5%
	Reward	0%	33%	88%	50%	0%	88%	88%	33%	0%	21%
	Mood	0%	45%	85%	65%	0%	85%	85%	55%	0%	25%
	Memory	5%	55%	100%	45%	0%	100%	100%	40%	0%	5%
	Anxiety	7%	21%	100%	71%	0%	100%	100%	50%	7%	50%
	Executive	0%	0%	88%	19%	0%	88%	88%	13%	0%	6%
	Front-Occ	0%	5%	60%	25%	0%	60%	60%	15%	5%	15%
	Facial Rec	13%	17%	83%	33%	0%	83%	83%	21%	8%	21%

the Chi Square is statistically significant at 70 % or higher. All networks exhibited a statistically significant Chi Square ($P < 0.05$), except for the fronto-occipital network.

Discussion

Surface EEG Paired t-Tests

Here we report results of this ENHANCE study, a prospective, Institutional Review Board-approved Study in healthy volunteers comparing a baseline EEG with an EEG after placement of a haptic vibrotactile trigger technology (VTT) embedded compression sleeve (eSmartr Smart Compression Sleeve) on the right or left forearm. There are no experimental variables associated with right- or left-handedness, and therefore the experimental results cannot be skewed by this unlimiting factor [1].

Over the past several years, research of haptic vibrotactile trigger technology (VTT) indicates that there are changes in EEG patterns for those patients exposed to VTT [1]. In addition, researchers have developed a deeper understanding of the multiple neural networks impacted by VTT and have developed related theories of how different brain regions interact with VTT [33,34,35]. The brain centers targeted by VTT have been shown to be responsive to external stimuli that incorporate the VTT technology and have produced positive outcomes in pain, sleep, balance, stability, fatigue, and with this report, a change in EEG data after placement of a compression sleeve with VTT were shown [3,8].

Ronald Melzack first proposed and hypothesized that networks of neurons communicating in "large loops", or through continuous cyclical processing, connect specific regions of the brain with the PNS during sensory processing [33]. He envisioned 3 distinct looping pathways: 1) a traditional sensory pathway with neural projections routed through the thalamus, 2) one that follows a path through the brainstem and parts of the limbic system, and 3) one associated with pathways that are routed through different Brodmann Areas (BA), particularly the somatosensory cortex. These loops were meant to explain the cognitive, emotional, and motor modalities through which humans experience sensations [33,34].

The EEG mapping of the pain neuromatrix, for instance, is corroborated with neuroimaging techniques such as functional analysis using magnetic resonance imaging (fMRI) in many experimental paradigms. The sensory patterns within the patches are in close symmetry between known EEG patterns and their role in modulating EEG and neuronal circuits within higher brain centers. [34].

This analytically innovative study of neural and cognitive networks shows a landscape of segregated yet integrated neuro-communication pathways potentially associated with an experimentally verified spectrum of EEG/qEEG patterns influenced by patterned tactile and somatosensory stimulations, using haptic vibrotactile trigger technology (VTT) and a VTT pattern named Cognitive Boost Technology (CBT) and tactile stimulatory trajectories [3].

Recent studies incorporating VTT technology for measuring somatosensory responses associated with cognitive networks [1,7,8,13] have shown positive outcomes in multiple disorders. The neuronal nexus connecting tactile mechanoreceptors in the forearm to the CNS with VTT and, by proxy, to the cognition networks is continuing to be explored.

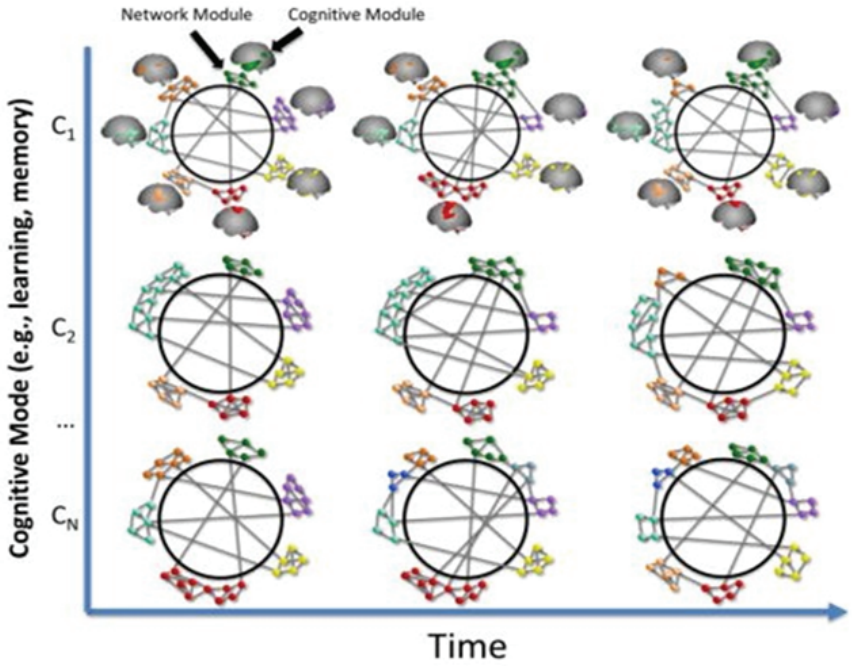

Figure 6. *Cognitive Model*

A Landscape of Cognitive Observations: Intricate Neuropathways and Regulatory Modules

The results of this study show that the EEG auto- and cross-spectrum is affected when a patterned eSmartr Smart Compression Sleeve is placed on a person's forearm as compared to a baseline EEG without wearing a VTT patterned sleeve. Interestingly, all twenty subjects involved in this study exhibited statistically significant changes in several brain networks, and group statistics were exceptionally significant for both the surface EEG power and LORETA current density in the alpha frequency band for 9 out of 10 networks [3,16,20,21].

This neural landscape is particularly consistent with recent scientific reports highlighting creative cognition and brain network dynamics across a wide spectrum of CNS modalities [4,36-38]. Furthermore, there are strikingly similar patterns of brain activity and connectivity across a wide range of creative tasks and behaviors that are consistent with specific EEG patterns [4]. As shown in this study, cognitions are crucial components in the integration of those neuropathways. In fact, the modulations induced by eSmartr somatosensory stimulations have direct implications for mapping interactive CNS networks in simulating complicated cognitive processes, including those pre-oriented with willful thoughts and decisions [1,39-41]. This technology should encourage further research and development of patterns that can directly interfere with the activities of cognition across specified time intervals [4]. The particular associations that are likely to exist between neural and cognitive modules have yet to be ascertained following the established observations reported in this study (see also the "Cognitive Model" in Figure-6).

Generally, the spectrum shows that there was a decrease in EEG absolute power in the alpha frequency band (8–12 Hz). Some reports have indicated that the reduction in alpha voltage is "associated with energy and cortical connectivity measures generated by event-related stimuli" [42]. In addition, there were bilateral hemispheric differences; however, the differences were strongest in the left hemisphere as compared to the right hemisphere. Physiologically, this appears to influence the verbal, analytical, and orderly expressions of the brain in a specified, pre-determined manner [1,3,4]. Surface EEG coherence demonstrated a hemispheric effect of "reduced connectivity" in the left fronto-occipital locations and "elevated coherence" in the right fronto-occipital locations. This indicates increased left hemisphere "differentiation" and increased right hemisphere "integration", which is corroborated by recent discoveries in cognitive science [1,4,12,43].

This segregation between left and right hemispheric localities suggests the involvement of cranial nerves that are closely associated with cognitive networks [43]. Although the eSmartr technology does not reveal which cranial nerves are ostensibly involved, it paves the way to create "parameterized computational models" (neuronal mapping) aimed at optimizing neuromodulatory pathways that may influence cognition in a specifically designed manner [4]. Perhaps the EEG patterns established following this stimulation may constitute an optimized mode for further analysis of those neurocircuits. The model therein suggested constitutes a modality that integrates somatosensation with central neural circuits projecting onto the cognitive networks across the CNS [1,4]. This is corroborated by a specific role for the posterior cingulate cortex that is active in cognition [44]. The involvement of the Brodmann areas, as established in this study, in modulating the axis of somatosensory-cognitive networks suggests a crucial role for the posterior cingulate cortex in determining attentional focus by "tuning brain metastability" spatially and temporally [4]. Interestingly, if this model is corroborated by further experimentation with this technology, then this technology could be used to evaluate 'enhanced' neuropathways while closely monitoring cognitive protocols [4,25,45-48].

The validation of the effects of the somatosensory arm stimulation on the CNS was further provided by the finding that LORETA current density consistently increased in the somatosensory projection areas on the medial surface of the somatosensory cortex. Bilateral frontal lobe Brodmann regions, particularly those in the left hemisphere, had the highest t-test differences (99.9 %) in the alpha frequency range (e.g., 8 Hz–12 Hz). The VTT embedded sleeve influenced electrical energy of the brain in the frontal, temporal, and parietal lobes. These findings correlate with the establishment of executive functions, especially at the level of the prefrontal cortex (PFC) [3,10,12,22,49,50]. It is well established that PFC networks are closely associated with the coordination of cognitive processes in both healthy and diseased states. This study suggests a possible link between PFC and cognition networks, given the dramatic variability in the alpha and beta frequencies of the brain EEG scans, which is consistent with other research [51], indicating these cognition networks are spatially and temporally flexible, exhibiting a certain degree of neuronal plasticity, reorganization, and learning processing [52]. This study has offered a platform to establish a basis for the integration of behavioral and cognitive networks [4].

Moreover, results indicated that the activity of the eSmartr sleeve correlates with reduced current density in the EEG in the default network that is involved in directed attention. The default network is considered most active when one is alone and ruminating on one's self-narrative and is inhibited when one attends to the concerns of the outside world [4,53,54]. The eSmartr sleeves can be interpreted to 'switch off' or 'minimize' one's self-narrative, which is necessary for paying attention to objects and occurrences in the external environment [4, 48,50].

The assumption of interference between external stimulations and EEG fluctuations that are likely involved with neuronal activities implicated in modulating human cognition is based on upon the understanding that exogenous neuronal stimuli can affect and change the patterns of EEG waveforms that create fluctuations and responses that are likely coordinated mechanically, sensorially, and cognitively in maintaining spatial, temporal, and dynamic somatosensory control pathways [1,3,4,8,20,25].

Recently, Thatcher et al. [20] specifically examined the neural mechanisms associated with the effects of somatosensory stimulation on the EEG patterns. Because those patterns are linked to human balance control and cognitive functions, there is compelling evidence that manipulating brain circuits can influence EEG waveform oscillations and, as a result, have sensory and motor-dependent consequences [3,8]. This is consistent with the observed effect of eSmartr somatosensory inputs on EEG patterns determined by changes in cognitive networks [4]. Results suggest that somatosensation via eSmartr sleeves, affects specific brain networks, modules, and cognits, which in turn can modulate the EEG patterns.

The Srysty Holdings Inc VTT-incorporated patterns are woven into performance products, such as socks, insoles, sleeves, and

patches, and designed to promote wellness by triggering neural pathways and circuits associated with the brainstem and other parts of the CNS, and that are crucially designed to control pain sensations, cognitive neurocircuits, and posture control, and also improve mindful cognition, balance, posture, mobility, and memory [6].

As noted, there is close symmetry between Srysty Holdings Inc technology and EEG patterns [1,16-19,23,55-56]. According to the study of Thatcher et al. [20] and current results, a sizeable and strong effect of the human performance technology (HPT) and VTT-patterned socks and eSmartr patterned sleeves with CBT on the EEG was present primarily in the theta, alpha, and beta frequency bands in varying degrees. The latter technology showed prominent alterations in the alpha and beta frequency bands. Anatomical validation was evident because of the strong effects on the homuncular projection of the feet and arm to the medial somatosensory cortex [1]. The precise mechanism of action of the VTT patterned technologies on the brain is still under investigation but has shown promising results in alleviating pain, improving sleep, reducing fatigue, maintaining balance, and improving cognitive perception [1,3,4,8,20].

There is mounting evidence to support enhanced brain activation mechanisms in "dynamic control tasks," irrespective of sensory, cognitive, or mechanical occurrences [57,58]. These "dynamic control tasks" are dual in nature given the fact that they are both sensory (visual, somatosensory, and vestibular) and mechanical (support surface translations) perturbations that correlatively circumvent sensory and motor responses emanating from any probable deficits [1,3,4,59].

Increasing research on VTT patterns and their effects on EEG is providing evidence-based, scientifically proven approaches to generating better balance and mobility, increased energy efficiency, enhanced pain management, improved sleep, reduced fatigue, faster recovery times, enhanced cognition abilities, and sustenance of neural health on the basis of modulating neural pathways associated with higher cognitive centers [4,47,60].

The theta, alpha, and beta networks associated with VTT and eSmartr and related technologies are crucial in facilitating somatosensory information processing during balance control, in addition to the integration, planning, and execution of motor-related responses emanating from cognitive centers [17,20,23,61,62]. Current advances in neurobiology states that cortical networks and pathways are crucial in determining the level of optimization necessary for cognitive control and the associated behavioral outcomes, which could be unraveled by partial directed coherence, a time-variant, frequency-selective, and directed functional connectivity analysis tool, such as the EEG protocols invested by human performance technology [1,4].

Evidence-Based Anatomy of eSmartr Manipulation of EEG Patterns Effectuated by Somatosensory Activation Pathways

Identifying the neuropathways activated by eSmartr technology is critical to understanding these outcomes. Here, the anatomy of this dimension is presented in support of potentially promising projections for enhancing neural circuits associated with cortical cognition, backed up by evidence provided by published studies in scientifically relevant fields [1,4,7,8,20.25].

Absolute Power Surface EEG

The relevance of the statistical differences between the recordings of subjects wearing the eSmartr-embedded sleeves in the "eyes closed" condition, as compared with the control group, indicates, at the very least, a potential activation of neural pathways within the brain that are being spatially and temporally identified and unraveled. Nevertheless, the involvement of both alpha and beta waveforms, as indicated, can shed important light on those possible pathways [1].

The observation of minimal alpha and beta frequency band oscillations, as compared with those of other frequencies, bears anatomical and physiological connotations backed up by scientific evidence [4,63]. For instance, most EEG recordings in various setups identified dramatic changes—usually downregulation—in the alpha and beta waveforms when cognition was involved [17,61,64,65]. In contrast, the theta waveforms were either unchanged or depressed, indicating independent mechanisms controlling their oscillations [1,3]. The observation that eSmartr depresses the alpha and beta band frequencies, especially in the left intra-hemispheric area and medial bank of the somatosensory cortex, highlights the possibility of somatosensory involvement that is likely to engage cognitions within the cerebellum, in particular; other neuronal pathways within higher centers of the brain are extremely likely. This is evidently backed up by several other reported experimental studies [15,25,66].

Surface EEG Coherence

The functional and anatomical connectivity in the human cortex are evidently dependent on neuronal oscillations [1,3,7,8]. The integrity of the functional connectivity in the human brain networks can then be assessed via the detection of synchronous neuronal activation, which can be captured by EEG [21,23,55,57,62,65].

The significant appearance of surface EEG coherence across various regions of the brain, in both the left and right hemispheres, provided compelling evidence for the presence of an intricate neuronal network [1,14]. This is corroborated by the observation that, with the exception of the delta frequency band in the T3-T4 region, other frequencies have been paired in both hemispheres [1,4].

The following observations, along with the following lines of scientific evidence, suggest that VTT embedded pattern sleeves can change EEG coherence patterns in a predetermined manner:

1. The somatosensory component of embedded eSmartr technology revealed patterns that are consistent with the haptic sensation and tactical perception theories [1,2,5]. Briefly, Reed and Ziat [5] state the following: "The haptic system uses the cutaneous and kinesthetic afferent subsystems to process the physical characteristics of objects and surfaces. The term "tactile perception", which refers to sensations obtained by touching objects in the external environment, is frequently used to describe the passive component of haptic perception. This tactile aspect of haptic perception is significantly influenced by the skin's mechanoreceptors and thermoreceptors (cutaneous inputs, for example). But haptic perception also covers active touch and the proprioceptive and kinesthetic signals that come from the stimulation of receptors in muscles, tendons, and joints. Based on the examination of perceptual and neurophysiological responses in both animals and humans, we have a better knowledge of the neural roots of haptic perception from the "skin to the brain". Evidently, haptic perception has features that are tightly linked to sensory, spatial, proprioceptive, and motor factors [3,5], all of which

are integral components of the eSmartr patterns, thereby bearing significant potential for applying the concept of haptic/tactual sensation to neuronal development, plasticity, and circuitry involved with human cognitive control, and perhaps with other mechanisms as well [1,7,8,11,67].

2. There have been circulating reports indicating that the EEG alpha band frequency falls as cognitive difficulty increases in central and parietal areas [63,66]. The embedded eSmartr sleeves caused oscillations in the alpha frequency in an analogous manner [1,20].
3. Similarly, other reports have indicated that bilateral alpha power reduction correlates with ratings of behavioral task difficulty [25,68]. Although the present study with embedded eSmartr does not corroborate this prior observation, it is likely that the reduction of the alpha and beta frequency bands in both hemispheres, particularly in the left hemisphere, is presumptuously associated with other tasks that might involve sensory or cognitive skills, which are to be ascertained [7,8].
4. It has been reported that frequency band coherence between central areas rises with increasing behavioral task difficulty [61,64,69]. The embedded experiment noticed a prominent reduction in EEG coherence across all frequency bands, indicating the possibility of the formation of intricate brain networks induced by this stimulation [20]. This might have ramifications for cognitive control and has been ascertained experimentally [1,4].
5. It has been observed that hemispheric asymmetry in theta and alpha/beta frequencies can be seen during continuous outcomes [15,63,70]. This asymmetry is observed in all frequencies in eSmartr, except the delta waveform, indicating possible involvement with specialized cognitive skills as well [1,20].
6. Finally, this asymmetry may suggest an active role for the non-dominant hemisphere in cognitive control [65]. The eSmartr experiment showed involvement of both hemispheres, albeit more prominent for the left hemisphere, indicating the presence of intricate pathways that may well exceed the dimension of localized cognition [1,3,4,7,8].

EEG coherence primarily decreased with eSmartr sleeves on in all of the frequency bands that were observed in both hemispheres. Decreased coherence, according to Thatcher et al. [20], indicates increased differentiation and increased complexity in brain networks.

The effects of eSmartr on the electrical energies of the brain were evident, especially in the left frontal and left temporal gyrus, the left anterior cingulate, and the left para-hippocampal gyrus. This corroborates with scientific reports providing evidence for the vital role of cortical circuits in EEG-recorded asymmetric oscillations in response to external stimuli [17,23,58,65,69].

These observations suggest that those activated Brodmann areas, particularly the anterior cingulate and para-hippocampal gyrus, are strongly associated with a host of cognitive functions, including attention allocation [1,3,7,8,17].

What is the putative connection between somatosensory stimulation caused by eSmartr-embedded sleeves and cognitive control? Research studies have unequivocally shown that the somatosensory system, as a complex system of sensory neurons and intricate pathways that respond to external or internal changes, is also involved in enhancing cognitive awareness by relaying information about stimulation factors to the brain, allowing it to activate the appropriate cognitive responses controlling decisions, attitudes, memories, and language skills [1,3,5,7,8,22].

The qEEG calculates voltage over frequency for the important regions of the brain using a mathematical process known as the spectral analysis or Fast-Fourier Transform (FTT) that has been used in our experimental setups with HPT and CBT [1]. The FFT generates a function that plots micro-voltage against frequency (see Figures 3 and 4).

A database that has been statistically normed to a population using a Gaussian distribution and Z-score is compared to this function, or FFT. Simply put, it can be said that a person has a performance improvement or deficit based on the comparison database if a known area of the brain differs from a specified Z-score by more than 2 Sigma [1]. Evidence provided indicates an FTT-dependent cognitive improvement with eSmartr technology over a specified period of time, an effect we have shown to be spatially and temporally oriented [1,3,7,8,71].

EEG Somatosensory Pathways and Haptic Vibrotactile Trigger Technology

EEG activity represents the geographically and temporally coordinated synchronous activity of many millions of cortical neurons. EEG analysis and interpretation require both art and science. The physiological variability of the typical EEG spans a wide range and is incredibly variable. This activity demonstrates the typical EEG waveforms and explains how the interprofessional team can better care for patients who are subject to EEG evaluation. This phenomenon is particularly enforced during the course of this experimentation with eSmartr, ensuring the validity and reproducibility of tangible, effectual results [7].

Clinical EEG's standard bandwidth concentrates on the examination of waveforms between 0.5 Hz and 70 Hz. The EEG recordings are bandpass filtered as part of this analysis. Clinical neurophysiologists and researchers have examined a wider EEG bandwidth, and have discovered that it can be clinically meaningful. A number of significant physiological and pathological aspects of brain activity are lost when the lower (infra-slow) or higher (ultra-fast) portions of the EEG frequency spectrum are eliminated from normal EEG. A full-bandwidth EEG (FbEEG) examines all of the waveforms that are physiologically and therapeutically significant without making any trade-offs that would prefer one frequency band over another [72]. However, it is uncommon in clinical practice to record EEG data at extremely high frequencies because doing so needs specialized equipment that can gather data at higher sampling rates, which in turn increases the amount of storage space required. This aspect has been carefully monitored in the eSmartr experiments, with an emphasis on the putative clinical somatosensory oscillations.

Data collected shows the following types of EEG waveforms can be distinguished based on the FbEEG recordings and according to an ascending hierarchy of oscillatory Hz ranges:

1. ***Infra-slow oscillations (ISO) (less than 0.5 Hz):*** ISOs, also known as spontaneous activity transients (SAT), are the dominant frequency in preterm infants, with frequencies as low as 0.01 to 0.1 Hz. At an early, immature stage, when sensory input plays a minor or no role in shaping neuronal connections, SATs represent endogenously

driven, spontaneous activity [73]. This particular aspect is independent of the observations therein reported by healthy adults. Additionally, non-REM sleep is accompanied by ISOs at a variety of frequencies (0.02 to 0.2 Hz), phase-synchronized with higher-frequency EEG activity [74]. The majority of low-frequency EEG research has concentrated on a variety of cognitive tasks and states, including motor motions (Bereitschafts potential), contingent stimulation (contingent negative variation, CNV), and the orienting paradigm [75,76]. These slow scalp potentials can last for many seconds and frequently have an amplitude of only a few microvolts, necessitating the use of FbEEG in addition to electrodes and skin-electrode connections with true DC characteristics for accurate recording. The link between somatosensory and very slow EEG responses as well as fluctuating low-frequency fluctuations at the cognitive focus has been demonstrated by invasive and non-invasive EEG monitoring in human and animal models [77]. Our eSmartr model is considered a typical demonstration of a non-invasive approach that could be developed into advanced technology for healthcare monitoring [1]. Recent evidence from non-invasive ictal DC recordings shows that focal onset modalities are correlated with protracted, comparatively high amplitude DC changes [78].

2. ***Delta (0.5 Hz–4 Hz):*** The fronto-central head areas of the body physically exhibit a strong delta rhythm during deep sleep. When there is localized brain dysfunction and widespread encephalopathy, a pathological delta rhythm appears in awake states. The absence of delta oscillations in eSmartr experimentation (the present work) and HPT [1,3] is consistent with an independent mechanism likely involved in somatosensory pathways during awake patterns. Adults experience frontal intermittent rhythmic delta activity (FIRDA), whereas children experience occipital intermittent rhythmic delta activity (OIRDA) [79]. In people with temporal lobe pathology, temporal intermittent rhythmic delta activity (TIRDA) is frequently observed [80]. As shown, the eSmartr-patterned sleeves have particularly affected the left frontal and left temporal surface EEGs, in addition to the medial bank of the somatosensory cortex in the alpha, and not the delta, frequency. This inconsistency with delta waveforms highlights the involvement of intermittent neuropathways in a delta-independent manner, the ramifications of which are under investigation.

3. ***Theta (4 Hz–7 Hz):*** This rhythm is induced by sleepiness as well as the N-1 and N-2 phases of early sleep. Due to early sleepiness, it is most noticeable in the fronto-central head regions and gradually migrates backward, replacing the alpha rhythm. In youngsters and young adults, elevated emotional states can also improve frontal rhythmic theta rhythm. The presence of focal theta activity when awake is indicative of focal brain impairment. Since the condition of experimental subjects in this study is a wake-conscience state, the absence of theta wave involvement is likely explained [1,20].

4. ***Alpha (8 Hz–12 Hz):*** In typical awake EEG recordings in the occipital head area, the posterior dominant alpha rhythm can be found. It is the distinguishing characteristic of the typical background rhythm captured by the adult EEG. In healthy people, the posterior rhythm reaches the alpha range of 8 Hz by the age of 3 and does not start to slow down until the ninth decade of life. In the general population, fast variations of the background alpha rhythm are observed. It is thought that a slowing of the background alpha rhythm indicates broad brain impairment [81]. Alpha rhythms have varying amplitudes in different people and at different times in the same person. The alpha rhythm is characterized by reactivity, which aids in identifying it. It is most easily seen when the eyes are closed and when the mind is at ease, and it is typically diminished by eye opening and mental effort. This corroborates our observation with the prominent defaults and network changes recorded with eSmartr technology in that particular eyes-closed condition. In addition, patients with diffuse encephalopathy may have generalized alpha activity, sometimes known as an "alpha coma", which is non-responsive to internal or external stimuli. Another alpha rhythm known as the mu rhythm manifests in the central head regions and has an arch-like form. When the contralateral limbs move or when you think about starting a movement, this pattern typically vanishes [82]. Although it is eye-opening, it is largely unchanged. Young adults are more likely to experience them than children or the elderly, where they are less common. Fatigue, sensory stimulation, and mental computation are attenuating factors. On both sides, they are very asymmetrical and asynchronous. This study has emphatically confirmed asymmetric and asynchronous oscillations with the alpha waveforms in subjects wearing the eSmartr sleeves as compared to non-patterned sleeves, indicating a key role for alpha waveforms in attenuating certain brain responses that are related to mental capacity and orientation [1,3,7,8].

5. ***Sigma:*** Sigma waves, also known as sleep spindles, are a physiological phenomenon that is observed in N-2 sleep. They are mainly noticeable in the fronto-central head areas and can be either sluggish (12 to 14 Hz) or fast (14 to 16 Hz) [83]. Spindle coma, or pathological spindle rhythm, is a symptom of widespread encephalopathy. The results therein reported cannot rule out the involvement of Sigma waveforms but have yet to be ascertained in separate experiments.

6. ***Beta (13 Hz–30 Hz):*** In healthy adults and children, the beta rhythm is the one that is most frequently observed. It is most pronounced in the frontal and central head areas and becomes less pronounced as it moves backward. Beta activity typically has an amplitude of 10 to 20 microvolts, seldom exceeding 30 microvolts. It frequently grows in amplitude during drowsiness and N-1 sleep before decreasing during N-2 and N-3 sleep. The majority of sedative drugs, including barbiturates, chloral hydrate, and benzodiazepines, boost beta activity in people's bodies [84]. It is possible for cortical injuries, abnormalities, and subdural, epidural, or subgaleal fluid collections to result in focal, regional, or hemispheric attenuation of beta. The attenuation of beta forms in eSmartr technology is consistent with a broad involvement of the frontal and temporal regions of the brain in conditions that are non-pathological. However, since our experiments were designed to unravel attenuation effects in both healthy and disease-stricken individuals to mediate improvements in cognition and other CNS functions, the variation in beta waveforms typically reinforces the notion that these EEG patterns are not biased or haphazard but rather outcomes of specific functionalities [3,7,8].

7. ***HFOs (high-frequency oscillations) at frequencies higher than 30 Hz:*** Gamma (30 to 80 Hz), ripples (80 to 200 Hz),

and fast ripples (200 to 500 Hz) are additional categories for these. Gamma rhythm has been linked to the integration of several sensory areas in perception. HFOs have been the subject of substantial research, especially in relation to cognition and neuropathological conditions. It is well known that cognitive foci produce extremely high-frequency activity [20]. Ultrafast frequency bursts (also known as fast ripples) have been observed in intracranial depth recordings from certain pathological conditions affecting the hippocampus (in both animal and human models), and these bursts likely correspond with the local clonogenicity of the brain tissue [85]. The location of a cognitive focus can also be determined by activity bursts at a comparatively lower frequency range (60 to 100 Hz), according to subdural recordings made during the presurgical examination of certain conditions [1]. Interictal HFOs may serve as indicators of human brain tissue that is attentive and decisive, according to the available evidence [1,3] and are further being explored. Interestingly, cognitive states and event-related potentials are correlated with ultrafast EEG activity. Gamma rhythms have a well-established role in a wide range of cognitive processes [86-88]. The category of ultrafast EEG signals known as brain stem evoked potentials (BERA) is well recognized and often measured. There have been reports of HFOs (more than 200 Hz) linked to somatosensory stimulation or motor movements, as well as their sensitivity to alertness states, motor interference, or pharmaceutical interventions like anesthetics or sedatives. These reports provide newer alternatives for brain monitoring and diagnostics [89,90]. They might aid in the early diagnosis of demyelination and other cortical integrity issues.

Currently, it is unclear exactly how the arm sleeve pattern affects the somatosensory system [3,7,8]. Although physiological, cellular, and molecular pathways are ostensibly involved [1,91-93], at least three evidence-based hypotheses are currently suggested: (1) The process of putting a sleeve on the forearm affects the EEG spectrum independently of the pattern; (2) dishabituation occurs due to the novelty of a sequence of edges stimulating the forearm; and (3) the specific properties and nature of the patterns making contact on the forearm are primarily responsible for the EEG effects. As noted, anatomical validation was visible due to the significant impacts on the homuncular projection of the arm to the medial somatosensory cortex in addition to the default network, as supported by a similar patterned technology [1,3,7,8].

Conclusion

Study results indicate that these non-pharmacologic, non-invasive, haptic vibrotactile trigger technology (VTT) embedded compression sleeves elicit a response in multiple neurological cognitive areas, especially the medial somatosensory cortex and default network, after EEG measurement. These networks play a key role in executive function, memory, attention, mood, and information flow. Results reported are very encouraging and suggest that the non-pharmacological compression sleeves with VTT have incredible potential to be added to the current approaches and treatments of noninvasive and nonpharmacological therapies with minimal side effects. Further evaluation, including more data from control and crossover groups are forthcoming and if validated, should encourage further research on VTT and its incorporation into additional products and add to the existing body of evidence that supports the use of this technology for those suffering from various disorders.

Acknowledgments

This IRB-approved study was funded by Srysty Holdings Inc.

Disclosure

John J. Haddad, Ph.D., received compensation for writing and for study interpretation. Mark DeBrincat, D.C., received compensation for his role as a site investigator. Duane M. North, Ph.D., received compensation for data review and study interpretation. Jay Dhaliwal, Eng. Physicist, was not compensated; he was an analytical reviewer for this research paper. Peter L Hurwitz is President of Clarity Science LLC and assisted in data review and manuscript development. The authors report no other disclosures.

References

1. Dhaliwal BS, Haddad J, Debrincat M, et al. Changes in Electroencephalogram (EEG) After Foot Stimulation with Embedded Haptic Vibrotactile Trigger Technology: Neuromatrix and Pain Modulation Considerations. Anesth Pain Res. 2022;6(2):1-11.
2. Fernandes AM, Albuquerque PB. Tactual perception: A review of experimental variables and procedures. Cogn Process. 2012;13(4):285-301.
3. Haddad JJ, Dhaliwal BS, Dhaliwal MS, Hurwitz P. Improvement in balance and stability using a novel sensory application: Haptic vibrotactile trigger technology. Int J Res Phys Med Rehabil. 2022;1(1):1-7
4. Medaglia JD, Lynall M-E, Bassett DE. Cognitive network neuroscience. J Cogn Sci. 2015;28(8):1471-1491.
5. Reed CL, Ziat M. Haptic perception: From the skin to the brain. In Reference Module in Neuroscience and Biobehavioral Psychology, Elsevier, 2018.
6. Westbrook CA, Dutcher J, Kusmierski S, Creswell JD, Akpan E, Hallion LS. Neural correlates of mindful disengagement from worry. J Psychopathol Clin Sci. 2023;132(1):38-50.
7. Doghramji P, Dietze D, Hurwitz P. Improving sleep and quality of life after use of a haptic vibrotactile trigger technology, drug-free, topical patch: Results from the HARMONI study. Int J Family Med Healthcare. 2023;2(1):1-7.
8. Gudin J, Dietze D, Dhaliwal G, Hurwitz P. Haptic vibrotactile trigger technology: Disrupting the neuromatrix to reduce pain severity and interference: Results from the HARMONI study. Anesth Pain Res. 2022;6(2): 1-7.
9. Julius D, Carlson JR. Editorial overview: Molecular biology of sensation. Curr Opin Neurobiol. 2015;34:v-vi.
10. Robertson D, Biaggioni I. (eds). Disorders of the autonomic system. Australia: Harwood Academic, 1995.
11. Yin J, Yuan Q. Structural homeostasis in the nervous system: A balancing act for wiring plasticity and stability. Front Cell Neurosci. 2015;8:439.
12. Park H-J, Friston K. Structural and functional brain networks: from connections to cognition. Science. 2013;342(6158):123841113.
13. Gudin J, Fason J, Hurwitz P. Reduction of Pain and Fatigue after Use of Over-The- Counter Socks Embedded With Haptic Vibrotactile Trigger Technology: Results from the Invigor Study. Int J Res Phys Med Rehabil. 2023;1(1):1-12.
14. Dhaliwal J. Internal research communication. VoxxLife, Inc., Toronto, Canada. 2018.
15. Sipp AR, Gwin JT, Makeig S, Ferris DP. Loss of balance during balance beam walking elicits a multifocal theta band electrocortical response. J Neurophysiol. 2013;110(9):2050-60.

16. Thatcher RW. Handbook of QEEG and EEG Biofeedback. Anipublishing, Inc., St. Petersburg, Florida, 2016.
17. Thatcher RW, Krause PJ, Hrybyk M. Cortico-cortical associations and EEG coherence: A two-compartmental model. Electroencephalogr Clin Neurophysiol. 1986;64(2):123-43.
18. Thatcher RW, North D, Biver C. Evaluation and validity of a LORETA normative EEG database. Clin EEG Neurosci. 2005;36(2):116-22.
19. Thatcher RW, North DM, Biver CJ. LORETA EEG phase reset of the default mode network. Front Hum Neurosci. 2014;8:529
20. Thatcher RW, DeBrincat M, North DM, Dhaliwal J. Effects of foot stimulation on the human electroencephalogram. Voxx HPT Clinical Studies, 2018.
21. Thatcher RW. Tomographic electroencephalography, magnetoencephalography. Dynamics of human neural network switching. J Neuroimaging. 1995;5(1):35-45.
22. Rubega M, Formaggio E, Di Marco R, et al. Cortical correlates in upright dynamic and static balance in the elderly. Sci Rep. 2021;11(1):14132.
23. Slobounov S, Hallett M, Stanhope S, Shibasaki H. Role of cerebral cortex in human postural control: An EEG study. Clin Neurophysiol. 2005;116(2):315-23.
24. Hata M, Kazui H, Tanaka T, et al. Functional connectivity assessed by resting state EEG correlates with cognitive decline of Alzheimer's disease – An eLORETA study. Clin Neurophysiol. 2016;127(2):1269-1278.
25. Mierau A, Pester B, Hülsdünker T, Schiecke K, Strüder HK, Witte H. Cortical correlates of human balance control. Brain Topogr. 2017;30(4):434-446.
26. Pascual-Marqui RD, Lehmann D, Koukkou M, et al. Assessing interactions in the brain with exact low-resolution electromagnetic tomography. Philos Trans A Math Phys Eng Sci. 2011;369(1952):3768-3784.
27. Zhang Y, Zhang J, Weng J. Dynamic Moore-Penrose inversion with unknown derivatives: Gradient neural network approach. EEE Trans Neural Netw Learn Syst. 2022a;PP.
28. Zhang W, Yang Y, Wu QMJ, Wang T, Zhang H. Multimodal Moore-Penrose inverse-based re-computation framework for big data analysis. IEEE Trans Neural Netw Learn Syst. 2022b;PP.
29. Lancaster JL, Woldorff MG, Parsons LM, et al. Automated Talairach atlas labels for functional brain mapping. Hum Brain Mapp. 2000;10(3):120-131.
30. Johnson CB, Schall M, Tennison ME, et al. Neocortical neuronal morphology in the Siberian Tiger (Panthera tigris altaica) and the clouded leopard (Neofelis nebulosa). J Comp Neurol. 2016;524(17):3641-3665.
31. Kawamura M. Korbinian Brodmann's scientific profile, and academic works. Brain Nerve. 2017;69(4):301-312.
32. Van den Heuvel MP, Hulshoff Pol HE. Exploring the brain network: A review on resting-state fMRI functional connectivity. Eur Neuropsychopharmacol. 2010;20(8):519-34.
33. Melzack R. Pain and the neuromatrix in the brain. J Dent Educ. 2001;65:1378-1382.
34. Derbyshire SWG. Exploring the pain "neuromatrix." Curr Rev Pain. 2000;4:467-477.
35. Mouraux A, Diukova A, Lee MC, et al. A multisensory investigation of the functional significance of the "pain matrix." Neuroimage. 2011; 54: 2237-2249.
36. Beaty RE, Benedek M, Silvia PJ, Schacter DL. Creative cognition and brain network Dynamics. Trends Cogn Sci. 2016;20(2):87
37. Higley MJ, Cardin JA. Spatiotemporal dynamics in large-scale cortical networks. Curr Opin Neurobiol. 2022;77:102627.
38. Valenti O, Mikus N, Klausberger T. The cognitive nuances of surprising events: Exposure to unexpected stimuli elicits firing variations in neurons of the dorsal CA1 hippocampus. Brain Struct Funct. 2018;223(7):3183-3211.
39. Filley CM, Fields RD. White matter and cognition: Making the connection. J Neurophysiol. 2016;116(5):2093-2104.
40. Loriette C, Ziane C, Ben Hamed S. Neurofeedback for cognitive enhancement and intervention and brain plasticity. Rev Neurol (Paris). 2021;177(9):1133-1144.
41. Uddin LQ. Cognitive and behavioral flexibility: neural mechanisms and clinical considerations. Nat Rev Neurosci. 2021;22(3):167-179.
42. Ehlers CL, Wills DN, Phillips E, Havstad J. Low voltage alpha EEG phenotype is associated with reduced amplitudes of alpha event-related oscillations, increased cortical phase synchrony, and a low level of response to alcohol. Int J Psychophysiol. 2015;98(1):65
43. Adair D, Truong D, Esmaeilpour Z, et al. Electrical stimulation of cranial nerves in cognition and disease. Brain Stimul. 2020;13(3):717-750.
44. Leech R, Sharp DJ. The role of the posterior cingulate cortex in cognition and disease. Brain. 2014;137(1):12-32.
45. Marshall K, Patapoutian A. Getting a grip on touch receptors. Science. 2020;368(6497):1311-1312.
46. Ouchi Y, Okada H, Yoshikawa E, Nobezawa S, Futatsubashi M. Brain activation during maintenance of standing postures in humans. Brain. 1999;122 (Pt 2):329-38.
47. Paquola C, Amunts K, Evans A, Smallwood J, Bernhardt B. Closing the mechanistic gap: the value of microarchitecture in understanding cognitive networks. Trends Cogn Sci. 2022;26(10):873-886.
48. Wolters AF, van de Weijer SCF, Leentjens AFG, Duits AA, Jacobs HIL, Kuijf ML. Resting-state fMRI in Parkinson's disease patients with cognitive impairment: A meta-analysis. Parkinsonism Relat Disord. 2019;62:16-27.
49. Menon V, D'Esposito M. The role of PFC networks in cognitive control and executive function. Neuropsychopharmacology. 2022;47(1):90-103.
50. Petersen SE, Sporns O. Brain networks and cognitive architectures. Neuron. 2015;88(1):207-19.
51. Hartwigsen G. Flexible redistribution in cognitive networks. Trends Cogn Sci. 2018;22(8):687-698.
52. Soto FA. Beyond the "conceptual nervous system": Can computational cognitive neuroscience transform learning theory? Behav Processes. 2019;167:103908.
53. Fox PT, Snyder AZ, Vincent JL, Corbetta M, Van Essen DC, Raichle ME. The human brain is intrinsically organized into dynamic, anticorrelated functional networks. Proc Natl Acad Sci USA. 2005;102(27):9673-9678.
54. Sridharan D, Levitin DJ, Menon V. A critical role for the right fronto-insular cortex in switching between central-executive and default mode networks. Proc Natl Acad Sci USA. 2009;105(34):12569-12574
55. Thatcher RW. EEG operant conditioning (biofeedback) and traumatic brain injury. Clin Electroencephalogr. 2000;31(1):38-4
56. Thatcher RW, North DM, Biver CJ. Diffusion spectral imaging modules correlate with EEG LORETA neuroimaging modules. Hum Brain Mapp. 2012;33(5):1062-75.
57. Slobounov S, Cao C, Jaiswal N, Newell KM. Neural basis of postural instability identified by VTC and EEG. Exp Brain Res. 2009;199(1):1-16.
58. Solis-Escalante T, van der Cruijsen J, de Kam D, van Kordelaar J, Weerdesteyn V, Schouten AC. Cortical dynamics during preparation and execution of reactive balance responses with distinct postural demands. Neuroimage. 2019;188:557-571.
59. Blakemore RL, Hyland BI, Hammond-Tooke GD, Anson JG. Distinct modulation of event-related potentials during motor

preparation in patients with motor conversion disorder. PLoS One. 2013;8(4):e62539.

60. Arshavsky YI. Neurons versus Networks: The Interplay between Individual Neurons and Neural Networks in Cognitive Functions. Neuroscientist. 2017;23(4):341-355.
61. Varghese JP, Staines WR, McIlroy WE. Activity in functional cortical networks temporally associated with postural instability. Neuroscience. 2019;401:43-58.
62. Thatcher RW, Biver CJ, North D. Spatial-temporal current source correlations and cortical connectivity. Clin EEG Neurosci. 2007;38(1):35-48.
63. Hülsdünker T, Mierau A, Strüder HK. Higher balance task demands are associated with an increase in individual alpha peak frequency. Front Hum Neurosci. 2016;9:695.
64. Tse YY, Petrofsky JS, Berk L, Daher N, Lohman E, Laymon MS, Cavalcanti P. Postural sway and rhythmic electroencephalography analysis of cortical activation during eight balance training tasks. Med Sci Monit. 2013;19:175-86.
65. Wittenberg E, Thompson J, Nam CS, Franz JR. Neuroimaging of human balance control: A systematic review. Front Hum Neurosci. 2017;11:170.
66. Edwards AE, Guven O, Furman MD, Arshad Q, Bronstein AM. Electroencephalographic correlates of continuous postural tasks of increasing difficulty. Neuroscience. 2018;395:35-48.
67. Tien, NW., Kerschensteiner, D. Homeostatic plasticity in neural development. Neural Dev. 2018;13,9.
68. Lehmann T, Büchel D, Cockcroft J, Louw Q, Baumeister J. Modulations of inter-hemispherical phase coupling in human single leg stance. Neuroscience. 2020;430:63-72.
69. Varghese JP, Beyer KB, Williams L, Miyasike-daSilva V, McIlroy WE. Standing still: Is there a role for the cortex? Neurosci Lett. 2015;590:18-23.
70. Solis-Escalante T, van der Cruijsen J, de Kam D, van Kordelaar J, Weerdesteyn V, Schouten AC. Cortical dynamics during preparation and execution of reactive balance responses with distinct postural demands. Neuroimage. 2019;188:557-571.
71. Brown JC, Goldszer IM, Brooks MC, Milano NJ. An Evaluation of the Emerging Techniques in Sports-Related Concussion. J Clin Neurophysiol. 2023;40(5):384-390..
72. Vanhatalo S, Voipio J, Kaila K. Full-band EEG (FbEEG): An emerging standard in electroencephalography. Clin Neurophysiol. 2005;116(1):1-8.
73. Vanhatalo S, Tallgren P, Andersson S, Sainio K, Voipio J, Kaila K. DC-EEG discloses prominent, very slow activity patterns during sleep in preterm infants. Clin Neurophysiol. 2002;113(11):1822-1825.
74. Vanhatalo S, Palva JM, Holmes MD, Miller JW, Voipio J, Kaila K. Infraslow oscillations modulate excitability and interictal epileptic activity in the human cortex during sleep. Proc Natl Acad Sci USA. 2004;101(14):5053-5057.
75. Birbaumer N, Elbert T, Canavan AG, Rockstroh B. Slow potentials of the cerebral cortex and behavior. Physiol Rev. 1990;70(1):1-41.
76. Cui RQ, Huter D, Egkher A, Lang W, Lindinger G, Deecke L. High resolution DC-EEG mapping of the Bereitschafts potential preceding simple or complex bimanual sequential finger movement. Exp Brain Res. 2000;134(1):49-57.
77. Ikeda A, Terada K, Mikuni N, et al. Subdural recording of ictal DC shifts in neocortical seizures in humans. Epilepsia. 1996;37(7):662-674.
78. Voipio J, Tallgren P, Heinonen E, Vanhatalo S, Kaila K. Millivolt-scale DC shifts in the human scalp EEG: evidence for a nonneuronal generator. J Neurophysiol. 2003;89(4):2208-2214.
79. Cordeau JP. Monorhythmic frontal delta activity in the human electroencephalogram: a study of 100 cases. Electroencephalogr Clin Neurophysiol. 1959;11:733-746.
80. Dalby MA. Epilepsy and 3 per second spike and wave rhythms. A clinical, electroencephalographic and prognostic analysis of 346 patients. Acta Neurol Scand. 1969:Suppl 40:3.
81. Aird RB, Gastaut Y. Occipital and posterior electroencephalographic rhythms. Electroencephalogr Clin Neurophysiol. 1959;11:637-656.
82. Chatrian GE, Petersen MC, Lazarte JA. The blocking of the rolandic wicket rhythm and some central changes related to movement. Electroencephalogr Clin Neurophysiol. 1959;11(3):497-510.
83. Gondeck AR, Smith JR. Dynamics of human sleep sigma spindles. Electroencephalogr Clin Neurophysiol. 1974;37(3):293-297
84. Frost JD, Carrie JR, Borda RP, Kellaway P. The effects of dalmane (flurazepam hydrochloride) on human EEG characteristics. Electroencephalogr Clin Neurophysiol. 1973;34(2):171-175.
85. Worrell G, Gotman J. High-frequency oscillations and other electrophysiological biomarkers of epilepsy: Clinical studies. Biomark Med. 2011;5(5):557-566.
86. Reiher J, Lebel M. Wicket spikes: Clinical correlates of a previously undescribed EEG pattern. Can J Neurol Sci. 1977;4(1):39
87. Tallon-Baudry C. Oscillatory synchrony and human visual cognition. J Physiol Paris. 2003;97(2-3):355-363.
88. Ward LM. Synchronous neural oscillations and cognitive processes. Trends Cogn Sci. 2003;7(12):553-559.
89. Haueisen J, Heuer T, Nowak H, et al. The influence of lorazepam on somatosensory-evoked fast frequency (600 Hz) activity in MEG. Brain Res. 2000;874(1):10-4.
90. Klostermann F, Gobbele R, Buchner H, Siedenberg R, Curio G. Differential gating of slow postsynaptic and high-frequency spike-like components in human somatosensory evoked potentials under isometric motor interference. Brain Res. 2001;922(1):95
91. Arshavsky YI. Cellular and network properties in the functioning of the nervous system: from central pattern generators to cognition. Brain Res Brain Res Rev. 2003;41(2-3):229-267.
92. Arshavsky YI. Neurons versus Networks: The Interplay between Individual Neurons and Neural Networks in Cognitive Functions. Neuroscientist. 2017;23(4):341-355.
93. Westmoreland BF, Klass DW. Unusual EEG patterns. J Clin Neurophysiol. 1990;7(2):209-228.